

# Activating Efficiency of $\text{Ca}^{2+}$ and Cross-Bridges As Measured by Phosphate Analog Release

Maki Yamaguchi and Shigeru Takemori

Department of Physiology, The Jikei University School of Medicine, Minato-ku, Tokyo 105-8461, Japan

**ABSTRACT** To assess the activating efficiency of  $\text{Ca}^{2+}$  and cross-bridges, the release rates of phosphate analogs from skinned fibers were estimated from the recovery of contractility and that of stiffness. Estimations were performed based on the assumptions that contractility was indicative of the population of analog-free myosin heads and that stiffness reflected the population of formed cross-bridges. Aluminofluoride (AlFx) and orthovanadate (Vi) were used as phosphate analogs with mechanically skinned fibers from rabbit psoas muscle. The use of the analogs enabled the functional assessment of activation level in the total absence of ATP. Fibers loaded with the analogs gradually recovered contractility and stiffness in normal plain rigor solution. The addition of  $\text{Ca}^{2+}$  to the plain rigor solution significantly accelerated their recovery, whereas ADP had no appreciable effect. ATP plus  $\text{Ca}^{2+}$  (contracting condition) accelerated the recovery by several tens of times. These results indicate that the cross-bridges formed during contraction have prominent activating efficiency, which is indispensable to attain full activation. A comparison between the activating efficiency evaluated from stiffness and that from contractility suggested that  $\text{Ca}^{2+}$  is more potent in accelerating the binding of actin to analog-bound myosin heads whereas cross-bridges mainly accelerate the subsequent analog-releasing step.

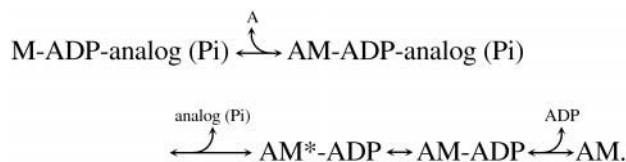
## INTRODUCTION

Several activators in addition to  $\text{Ca}^{2+}$  are known for skeletal muscle. For instance, myofilaments of skeletal muscle contract even in the absence of  $\text{Ca}^{2+}$  at low  $[\text{MgATP}]$  and at high  $[\text{MgADP}]$  exceeding  $[\text{MgATP}]$  (Bremel and Weber, 1972; Shimizu et al., 1992). These  $\text{Ca}^{2+}$ -independent contractions have been ascribed to the cooperative activating effects of strongly bound complexes of actomyosin (AM; cross-bridges) such as AM and AM-ADP. In addition, recent observations of the binding of fluorescent S1 to rigor myofibrils (Swartz et al., 1996) and the translocation of tropomyosin in the groove along the thin filament (Vibert et al., 1997) have shown that without the binding of myosin heads to the thin filament  $\text{Ca}^{2+}$  cannot induce full activation. These imply that the cooperative activating effects of cross-bridges formed during contractile actomyosin-ATPase cycling (contractile cross-bridges) is essential to the maximal activation of skeletal muscle even in the physiological contraction.

Concerning the activating efficiency of the actomyosin complexes, several researchers discussed the activating effect of AM-ADP on the myofilament compared with AM. For example, experiments with caged-ATP and apyrase have shown that the presence of MgADP considerably enhances transient contraction during the transition from the rigor to relaxed state in skinned fibers (Thirlwell et al., 1994). However, the transient and complex nature of this

contraction made a quantitative estimate of the activating efficiency of AM and AM-ADP difficult (Horiuti et al., 1997). The estimate requires the proportion of each cross-bridge state to be known. For the same reason, the cooperative activating effect exerted by the contractile cross-bridges is hard to distinguish from that of other activating factors such as  $\text{Ca}^{2+}$  coexisting in ordinary contractions.

Aluminofluoride (AlFx) as well as orthovanadate (Vi) is a well-established analog of inorganic phosphate ( $\text{P}_i$ ), which forms a stable complex of M-ADP-analog only during active ATPase cycling in skinned fibers (Takemori et al., 1995a; Chase et al., 1994; Danzig and Goldman, 1985). The dissociation of the complex is documented to follow a mechanism analogous to the commonly postulated mechanism for the physiological  $\text{P}_i$  release from M-ADP- $\text{P}_i$ ; that is,



As the activation of the myofilaments has been shown to facilitate the process as well as the physiological  $\text{P}_i$ -release process (Chase et al., 1994; Danzig and Goldman, 1985), one could consider the release rate of analog from the M-ADP-analog complex to be one index of the activation level of the skinned fiber.

In the present study, we aimed to determine the relative activating efficiencies of various cross-bridges and of  $\text{Ca}^{2+}$  from the release rates of Vi and AlFx from skinned fibers. The release rates were estimated from the recovery of contractility and stiffness of the fibers. The stability of M-ADP-Vi and M-ADP-AlFx allowed us to measure the

Received for publication 4 February 2000 and in final form 28 September 2000.

Address reprint requests to Dr. Maki Yamaguchi, Department of Physiology, The Jikei University School of Medicine, Minato-ku, Tokyo 105-8461, Japan. Tel.: 81-3-3433-1111; Fax: 81-3-3431-3827; E-mail: maki@jikei.ac.jp.

© 2001 by the Biophysical Society

0006-3495/01/01/01/371/08 \$2.00

analog-releasing process in the total absence of MgATP. The advantage of such a procedure is that, without ATPase cycling, one can assume each population of myosin heads to be in one of the states from M-ADP-analog to AM in the above scheme.

## MATERIALS AND METHODS

### Solutions

Solution composition is listed in Table 1. All of the solutions were designed using stability constants reported by Smith and Martell (1974–1982). Ionic strength was adjusted to 0.20 M and pH to 7.0 at 20°C in common.

Relaxing,  $\text{Ca}^{2+}$ -activating, and analog-loading solutions were estimated to contain 3.5 mM MgATP.  $[\text{Ca}^{2+}]$  of  $\text{Ca}^{2+}$ -activating and  $\text{Ca}^{2+}$ -rigor solutions was estimated to be  $10^{-4.4}$  M. The Vi-loading solution was prepared by adding 1 mM Vi (prepared according to the method of Danzig and Goldman, 1985), and the AlFx-loading solution by adding 0.5 mM  $\text{Al}(\text{NO}_3)_3$  together with 10 mM NaF (which yields 0.5 mM AlFx according to Chase et al., 1993), to the  $\text{Ca}^{2+}$ -activating solution. In the Vi- and AlFx-loading solutions, pH was readjusted with 1 N KOH and 1 N methanesulfonate, respectively, after the addition of the analogs. These analog additions and the subsequent pH adjustments affected the ionic strength of the solution by no more than 10 mM, an effect considered to be negligible in the present analyses.

With the exception of the ADP-rigor solution, all the rigor solutions contained 1 U/ml apyrase (Sigma, St. Louis, MO) to remove contaminant ATP and ADP.  $[\text{MgADP}]$  of the ADP-rigor solution was estimated to be 0.4 mM, which is enough to saturate myosin heads (Danzig et al., 1991; Shoenberg and Eisenberg, 1987). ADP-rigor solution contained 0.2 mM P-P-diadenosine pentaphosphate (Sigma) to inhibit myokinase and 1 U/ml hexokinase plus 0.6 mM glucose to remove contaminant ATP. When stiffness of a fresh fiber was measured as a control, 20 mM 2,3-butanedione monoxime (BDM; Nacalai Tesque, Tokyo, Japan) was initially added to the plain rigor solution to suppress rigor tension development.

### Tension and stiffness measurements

All the experiments were performed at 20°C. Skinned fibers were prepared by mechanical peeling of the sarcolemma from single fibers of the psoas muscle of the rabbit (Natori, 1954). To destroy internal membranous structures, each fiber was rinsed with relaxing solution containing 0.5% Triton X-100 for 15 min before use.

To measure tension, the thermoregulated bubble plate system similar to that described by Horiuti (1986) was used. The system was equipped with both UL-2 (Minebea, Tokyo, Japan) and 403A (Cambridge Technology,

Cambridge, MA) tension transducers. Sarcomere spacing was set at 2.5  $\mu\text{m}$  using the He-Ne laser diffraction technique.

Stiffness measurements were performed on the stage of a microscope with the aid of a piezo-actuator (LVPZ Translator, Physik Instrumente, Waldbronn, Germany) driven by an LVPZ Power Amplifier (E501, Physik Instrumente). One end of the fiber was oscillated sinusoidally at 500 Hz by the piezo-actuator at an amplitude of 0.1–0.2% of the fiber length. The resulting force oscillation detected at the other end of the fiber by a force transducer (AE801, SensoNor, Horten, Norway) was separated into in-phase and out-of-phase (quadrature) components using a lock-in-amplifier (5610B, NF-Electronics Instrument, Yokohama, Japan). The in-phase stiffness will be simply referred to hereafter as stiffness.

## RESULTS

### Recovery of contractility of analog-loaded fibers

Fig. 1 illustrates a standard protocol used to observe the recovery of contractility in a fiber preloaded with a  $\text{P}_i$  analog. First, the fiber was activated in the analog-loading solution (Aa) to introduce the analog into the fiber. After a small initial active tension had decayed almost exponentially within 1 min to a steady level of 2–3% of the original maximal  $\text{Ca}^{2+}$ -activated tension, the fiber was transferred to the relaxing solution (Lx) to wash the analog out of the fiber. According to Danzig and Goldman (1985) the analog molecules were specifically trapped on the majority of the myosin heads to form stable M-ADP-analog complexes with this procedure. Then the fiber was preincubated successively in the plain rigor solution for 3.75 min (Gp) and the  $\text{Ca}^{2+}$ -rigor solution (Gc) for 0.25 min to deplete ATP in the fiber before the incubation in the test rigor solution (Gt) for a given period of time. If the test solution deregulates the thin filament to accelerate dissociation of the M-ADP-analog complex, the recovery of contractility takes place. Finally, to assess contractility, the fiber was activated in the analog-free  $\text{Ca}^{2+}$ -activating solution (Ap). An instantaneous tension development was followed by a gradual creep of tension toward the original maximal level.

In the following subsection, we adopted the recovery rates of contractility as an index of the activating efficiency of the test rigor solution. Contractility was measured by the instantaneous tension development upon  $\text{Ca}^{2+}$  activation,

**TABLE 1** Solutions

	Concentration (in mM)									
	$\text{Na}_2\text{ATP}$	Mg (MS) <sub>2</sub>	EGTA	PIPES	K (MS)	CP	Ca (MS) <sub>2</sub>	KADP	Vi	Al (NO <sub>3</sub> ) <sub>3</sub>
Plain rigor		1.9	10	20	127					
ADP-rigor		2.4	10	20	123			1.0		
$\text{Ca}^{2+}$ -rigor		1.5	10	20	108		9.9			
$\text{Ca}^{2+}$ -activating	4.3	5.6	10	20	55	10	10			
Relaxing	4.2	6.0	10	20	75	10				
Vi-loading	4.3	5.6	10	20	55	10	10		1.0	
AlFx-loading	4.3	5.6	10	20	55	10	10			0.5
										10

MS, methanesulfonate; CP indicates creatine phosphate.

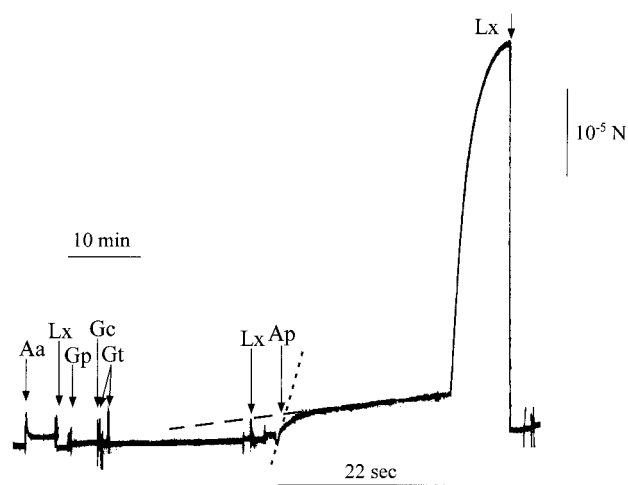


FIGURE 1 A typical tension trace showing the  $\text{Ca}^{2+}$  activation of the analog-loaded fiber after incubation in the test rigor solution. After the loading of AIFx in the AIFx-loading solution (Aa), the fiber relaxed in the analog-free relaxing solution (Lx) and was successively transferred to a series of rigor solutions: plain rigor solution (Gp),  $\text{Ca}^{2+}$ -rigor solution (Gc), and test rigor solution (Gt; plain rigor solution in this particular case). Contractility of the fiber was then measured by the instantaneous tension development in the  $\text{Ca}^{2+}$ -activating solution (Ap). Note the expanded time scale for the initial part of the contraction indicated by the solid bar below the trace. The instantaneous tension level upon  $\text{Ca}^{2+}$  activation was conveniently defined as the height of the intercepting point of the initial steepest tangential line (dotted line) and the following asymptotic line (dashed line).

whose level was defined as the tension level of the intercepting point of the steepest tangential line and the following asymptotic line as shown in Fig. 1.

### Recovery rates of contractility

Right after the successive preincubation in the plain and  $\text{Ca}^{2+}$ -rigor solutions, contractility measured by the instantaneous tension developed on  $\text{Ca}^{2+}$  activation was  $\sim 15 \pm 4\%$  ( $n = 3$ ) of the maximal tension in AIFx-loaded fibers and  $39 \pm 6\%$  ( $n = 5$ ) in Vi-loaded fibers (see the intercept at time 0 in Fig. 2). On the assumption that contractility is in proportion to the population of analog-free myosin heads,  $\sim 15\%$  of myosin heads in the AIFx-loaded fibers and  $40\%$  in the Vi-loaded fibers formed rigor cross-bridges at the beginning of the incubation in the test rigor solution.

Although no increase in tension was observed during the incubation in any of the rigor solutions (cf. Fig. 1), contractility gradually recovered as a function of the duration of the incubation period (Fig. 2 A). For comparison, the recovery rates of contractility in the relaxing and  $\text{Ca}^{2+}$ -activating solutions were also measured in the same manner as in the case for the test rigor solutions.

The comparison of the whole recovery processes in AIFx-loaded fibers clearly indicates the followings. First, MgADP in the ADP-rigor solution did not accelerate the recovery of

contractility in the plain rigor solution. Second,  $\text{Ca}^{2+}$  in the  $\text{Ca}^{2+}$ -rigor solution markedly accelerated the recovery. And third, the recovery rate in the  $\text{Ca}^{2+}$ -rigor solution was still considerably slower than that in the  $\text{Ca}^{2+}$ -activating solution.

The Vi-loaded fibers recovered contractility in the plain rigor solution with a time course similar but about several times faster than that of AIFx-loaded fibers (Fig. 2 B). In Vi-loaded fibers, as in AIFx-loaded fibers,  $\text{Ca}^{2+}$  but not ADP accelerated the recovery of contractility although the rate in the  $\text{Ca}^{2+}$ -rigor solution was far slower than that in the  $\text{Ca}^{2+}$ -activating solution.

To assign activating efficiency to various species of cross-bridges and  $\text{Ca}^{2+}$ , the recovery rate of contractility for the initial linear part of the recovery process in each test condition was obtained (Table 2). We determined the rate for each test condition as the slope of the tangential line drawn by eye to the initial linear part of the averaged recovery process (shown in Fig. 2). The linear parts we have chosen were the initial 40 min for rigor and ADP-rigor, 5 min for  $\text{Ca}^{2+}$ -rigor, 2.5 min for  $\text{Ca}^{2+}$  activation, as for AIFx, 10 min for rigor and ADP-rigor, 5 min for  $\text{Ca}^{2+}$ -rigor, and 0.5 min for  $\text{Ca}^{2+}$  activation, as for Vi. The relative recovery rates of contractility in the format of plain rigor/ADP-rigor/ $\text{Ca}^{2+}$ -rigor/ $\text{Ca}^{2+}$ -activating came to be 1/0.8/5/40 for AIFx and 1/1/2/40 for Vi. These rates are considered to represent relative efficiency of the activators in each condition, that is AM, AM-ADP,  $\text{Ca}^{2+}$  plus AM, and  $\text{Ca}^{2+}$  plus contractile cross-bridges.

### Recovery rates of stiffness

As shown in the scheme in the Introduction, the accelerated dissociation of M-ADP-analog in activated myofibrils would begin with the formation of an AM-ADP-analog complex. If an activator accelerates the formation of AM-ADP-analog complex more than the subsequent analog-releasing step, myosin heads may recover an affinity to actin well before they recover contractility. From this viewpoint, stiffness measurements were performed on AIFx-loaded fibers. If the AM-ADP-analog complex contributes significantly to fiber stiffness, then the recovery of stiffness would precede that of contractility.

Fig. 3 A shows the representative traces of tension and stiffness during the loading of AIFx and the subsequent incubation in the plain rigor solution. In the AIFx-loading solution, fiber stiffness as well as active tension rapidly decreased to a steady level within 1 min. As long as the fiber had been incubated in the relaxing solution after the loading of AIFx, stiffness in the plain rigor solution was initially suppressed. This confirms the stability of M-ADP-AIFx complexes formed in the AIFx-loading solution.

When the recovery of rigor stiffness in a test rigor solution was to be examined, AIFx-loaded fibers were preincubated in the plain rigor solution before the incubation in the

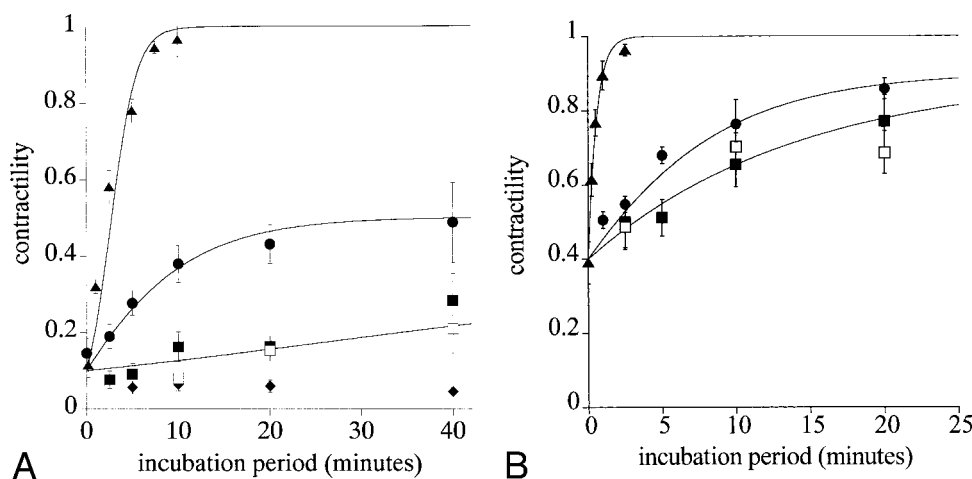


FIGURE 2 (A) Recovery of contractility of AIFx-loaded fibers with incubation in various test rigor solutions. The ordinate of the relation shows the size of the instantaneous tension upon  $\text{Ca}^{2+}$  activation relative to the original maximal  $\text{Ca}^{2+}$ -activated tension. The abscissa shows the incubation period in various test solutions.  $\bullet$ ,  $\square$ , and  $\blacksquare$ , respectively, the averaged results for the incubation in  $\text{Ca}^{2+}$ -rigor ( $n = 5, 8, 9, 9$ , and  $7$  for the data at  $2.5, 5, 10, 20$ , and  $40$  min, respectively), ADP-rigor ( $n = 5, 5$ , and  $5$  for the data at  $10, 20$ , and  $40$  min, respectively), and plain rigor ( $n = 3, 5, 5, 6, 5$ , and  $5$  for the data at  $0, 2.5, 5, 10, 20$ , and  $40$  min, respectively) solutions. The recovery processes of contractility after the incubation in relaxing ( $\blacklozenge$ ;  $n = 5, 5, 5$ , and  $5$  for the data at  $5, 10, 20$ , and  $40$  min, respectively) and  $\text{Ca}^{2+}$ -activating ( $\blacktriangle$ ;  $n = 3, 5, 16, 12, 3$ , and  $5$  for the data at  $0.17, 1, 2.5, 5, 7.5$ , and  $10$  min, respectively) solutions are also shown. Bars represent  $\pm$ SEM. The curves were drawn arbitrarily. Activating efficiency was estimated from the slope of lines tangential to the initial part of the curve (see Table 2; the lines are not shown in the figure). (B) Recovery of contractility of Vi-loaded fibers with incubation in various test solutions. The ordinate of the relation shows the size of the instantaneous tension upon  $\text{Ca}^{2+}$  activation relative to the original maximal  $\text{Ca}^{2+}$ -activated tension. The abscissa shows the incubation period in various test solutions.  $\bullet$ ,  $\square$ , and  $\blacksquare$ , respectively, the averaged results for the incubation in  $\text{Ca}^{2+}$ -rigor ( $n = 4, 9, 4, 5$ , and  $3$  for the data at  $1, 2.5, 5, 10$ , and  $20$  min, respectively), ADP-rigor ( $n = 6, 5$ , and  $7$  for the data at  $2.5, 10$ , and  $20$  min, respectively), and plain rigor ( $n = 5, 5, 7, 4$ , and  $3$  for the data at  $2.5, 5, 10, 20$ , and  $40$  min, respectively) solutions. The recovery process of contractility after the incubation in  $\text{Ca}^{2+}$ -activating solution ( $\blacktriangle$ ;  $n = 5, 7, 13, 5, 5$  for the data at  $0, 0.25, 0.5, 1, 2.5$  min, respectively) is also shown. Bars represent  $\pm$ SEM. The curves were drawn arbitrarily.

test rigor solution. After the initial rapid increase, stiffness continued to increase during the preincubation period (stiffness recovery). The process of stiffness recovery gradually

TABLE 2 Recovery rates of contractility and stiffness

	Contractility (/second)		Stiffness (/second)
	AIFx*	Vi†	AIFx‡
Plain rigor	$8.6 \times 10^{-5}$	$4.6 \times 10^{-4}$	$2.1 \times 10^{-4}$
ADP-rigor	$6.9 \times 10^{-5}$	$3.5 \times 10^{-4}$	$2.6 \times 10^{-4}$
$\text{Ca}^{2+}$ -rigor	$4.3 \times 10^{-4}$	$7.6 \times 10^{-4}$	$1.8 \times 10^{-3}$
$\text{Ca}^{2+}$ -activating	$3.3 \times 10^{-3}$	$1.5 \times 10^{-2}$	$3.7 \times 10^{-3}$

Contractility is dimensionless because it is expressed relative to the original level before the loading of the analog. Stiffness is expressed relatively and thence dimensionless. Stiffness in rigor condition is expressed relative to the plateau level attained with prolonged incubation in  $\text{Ca}^{2+}$ -rigor solution, and stiffness in  $\text{Ca}^{2+}$ -activating solution is expressed relative to its final plateau level.

\*Correlation coefficients of the linear fitting were  $0.943$  ( $n = 5$ ),  $0.946$  ( $n = 3$ ),  $0.953$  ( $n = 3$ ), and  $0.989$  ( $n = 3$ ) for rigor, ADP-rigor,  $\text{Ca}^{2+}$ -rigor, and  $\text{Ca}^{2+}$ -activating solutions, respectively.

†Correlation coefficients of the linear fitting were  $0.927$  ( $n = 3$ ),  $0.988$  ( $n = 3$ ), and  $0.958$  ( $n = 3$ ) for rigor,  $\text{Ca}^{2+}$ -rigor, and  $\text{Ca}^{2+}$ -activating solutions, respectively. The slope for ADP-rigor was obtained from two data points.

‡SEMs were  $2.7 \times 10^{-5}$  ( $n = 19$ ),  $5 \times 10^{-5}$  ( $n = 6$ ),  $2.3 \times 10^{-4}$  ( $n = 19$ ), and  $1.1 \times 10^{-3}$  ( $n = 6$ ) for rigor, ADP-rigor,  $\text{Ca}^{2+}$ -rigor, and  $\text{Ca}^{2+}$ -activating solutions, respectively.

attained an almost steady rate by 15 min. The fiber was then transferred to the test rigor solution. Upon transfer to the  $\text{Ca}^{2+}$ -rigor solution, the recovery rate of stiffness was accelerated by  $8.6 \pm 1.1$  times (mean  $\pm$  SEM;  $n = 19$ ; Fig. 3 B; Table 2). Fiber transfer from the plain rigor solution to the ADP-rigor solution induced an instantaneous drop in stiffness by  $\sim 15 \pm 4.5\%$  ( $n = 11$ ) without an appreciable change in the recovery rate (ADP accelerated the rate by  $1.2 \pm 0.2$  times;  $n = 6$ ; Fig. 3 C).

The stiffness recovery in any of the rigor solutions was considerably slower than that in the  $\text{Ca}^{2+}$ -activating solution (Fig. 3 D). The final stiffness level attained with a prolonged incubation in rigor solutions was somewhat lower than that in the  $\text{Ca}^{2+}$ -activating solution (Fig. 3, B and D). As the AIFx-loaded fibers developed little tension in the rigor solutions, the smaller final stiffness could be due to the larger attenuating effect of less strained compliant components serial to cross-bridges. To test this possibility, we put fresh fibers into rigor with or without tension development (data not shown). When rigor was induced in the presence of 20 mM butanedione monoxime (BDM), rigor tension development was almost completely suppressed. In this case, rigor stiffness was significantly smaller ( $\sim 60\%$ ) than the stiffness in the  $\text{Ca}^{2+}$ -activating solution. The removal of BDM after the induction of rigor did not affect the stiffness. On the other hand, when rigor was induced with



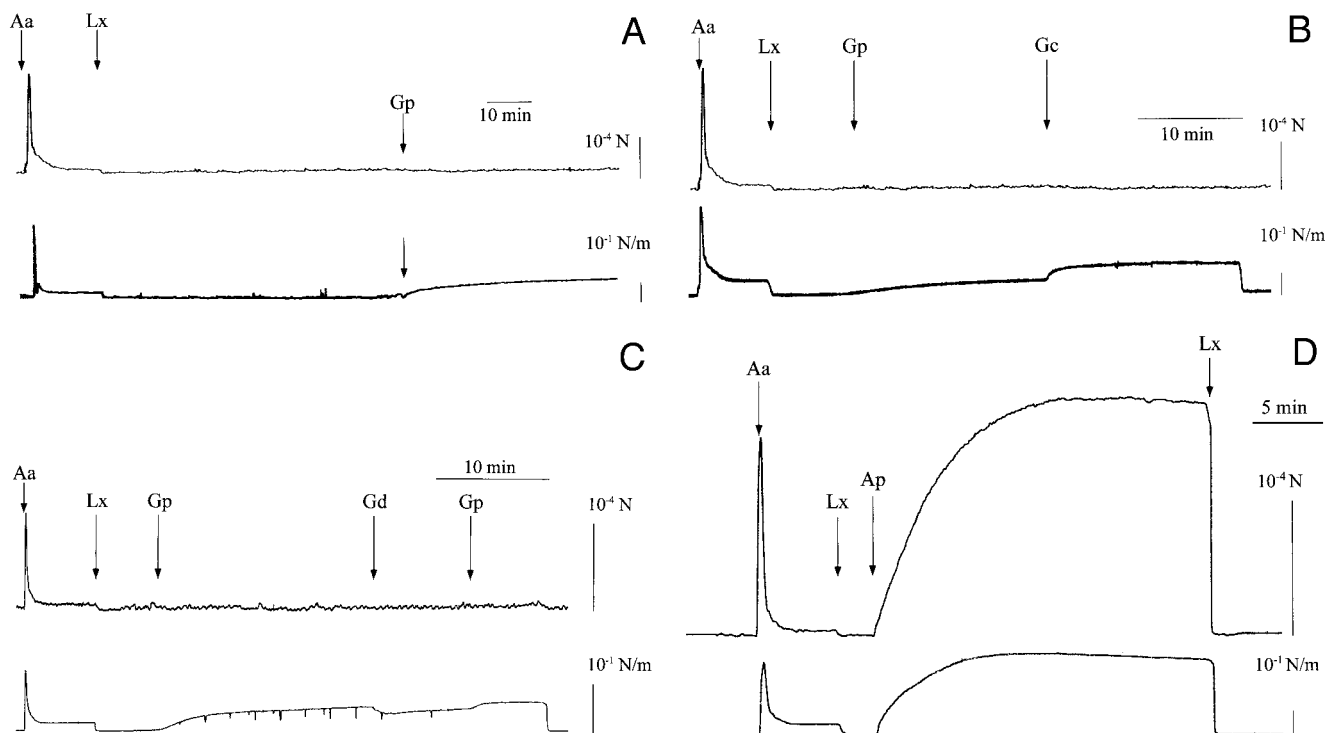


FIGURE 3 (A) Recordings of tension (upper trace) and stiffness (lower trace) of an AIFx-loaded fiber. The loading of AIFx was performed with the contraction in the AIFx-loading solution (between the arrows labeled Aa and Lx). At the arrow labeled Gp the fiber was put into the plain rigor solution, in which recovery of stiffness was observed. (B) Recordings of tension (upper trace) and stiffness (lower trace) of an AIFx-loaded fiber during the incubation in plain rigor and  $\text{Ca}^{2+}$ -rigor solution. After the loading of AIFx into the fiber as in Fig. 3 A (between the arrows labeled Aa and Lx) the fiber was placed first into the plain rigor (Gp) and then into the  $\text{Ca}^{2+}$ -rigor solution (Gc). (C) Recordings of tension (upper trace) and stiffness (lower trace) of an AIFx-loaded fiber during the successive incubation in plain rigor and ADP-rigor solution. After the loading of AIFx into the fiber as in Fig. 3 A (between the arrows labeled Aa and Lx) the fiber was placed successively into the plain rigor (Gp) and then the ADP-rigor (Gd) and back to the plain rigor solution (Gp). (D) Recordings of tension (upper trace) and stiffness (lower trace) of an AIFx-loaded fiber in the  $\text{Ca}^{2+}$ -activating solution. After the loading of AIFx into the fiber as in Fig. 3 A (between the arrows labeled Aa and Lx) the fiber was directly transferred to the  $\text{Ca}^{2+}$ -activating solution (Ap).

rigor tension development in the absence of BDM, larger rigor stiffness was observed. When rigor was induced at the maximal active tension level by transferring the fiber from  $\text{Ca}^{2+}$ -activating solution to the  $\text{Ca}^{2+}$ -rigor solution, stiffness markedly increased (up to 280% of the stiffness in the  $\text{Ca}^{2+}$ -activating solution) with the progress of rigor induction. Therefore, we concluded that the final stiffness level recovered in the rigor solutions was significantly attenuated by the larger serial compliance.

## DISCUSSION

### Rigor tension during analog release process

Rigor tension increase was not detected during the incubation periods in the test rigor solutions whereas stiffness steadily recovered. This finding indicates that, unlike  $\text{P}_i$  release in the physiological actomyosin ATPase cycle, the release of the  $\text{P}_i$ -analogs from actomyosin is not coupled with tension generation. In addition, this indicates that the formation of rigor cross-bridges does not necessarily accompany force development in the complete absence of

MgATP. Ordinary rigor tension would be, therefore, accumulated strain imposed on rigor cross-bridges by  $\text{Ca}^{2+}$ -independent contraction at the depleting concentration of MgATP during the transition to the rigor state. This is compatible with the finding that rigor tension amplitude depends markedly on the procedure inducing the fiber into the rigor state (Takemori et al., 1995b).

### Stiffness decrease induced by ADP

One may consider that the decrease in measured stiffness of the AIFx-loaded fibers upon transfer to the ADP-rigor solution (Fig. 3 C) reflects a change in the population of AM-ADP-AIFx complexes that contributes to stiffness. However, this is not likely to be the case because the withdrawal of ADP reversed the decrease (Fig. 3 C) and the dissociation of  $\text{P}_i$  analogs from the complexes is considered to precede that of ADP (Beck et al., 1992; Danzig and Goldman, 1985; Maruta et al., 1993).

We consider the decrease to be due to the binding of MgADP to AM. In rigor skinned fibers, which had no

analog, ADP is reported to induce reversible decreases in tension and stiffness (Danzig et al., 1991; Marston et al., 1976; Shoenberg and Eisenberg, 1987) through a conformational change in myosin heads (Takemori et al., 1995b).

### **Ca<sup>2+</sup> and rigor cross-bridges fail to attain full activation**

The recovery rates of contractility obtained with Vi were several times larger than those corresponding rates obtained with AIFx. This is consistent with the finding of Chase et al. (1994) of a recovery rate of the Ca<sup>2+</sup>-activated force in Vi-loaded skinned fibers three times faster than that in AIFx-loaded fibers. Despite this difference in the absolute values, relative recovery rates of contractility for AIFx (plain rigor/ADP-rigor/Ca<sup>2+</sup>-rigor/Ca<sup>2+</sup>-activating = 1/0.8/5/40) and Vi (1/1/2/40) showed general characteristics in common that could be summarized as follows. First, the activating efficiency of AM-ADP (in ADP-rigor) is not appreciably higher than that of AM (in plain rigor), and second, the Ca<sup>2+</sup> and rigor cross-bridges (AM and AM-ADP) fail to attain the activation level in the Ca<sup>2+</sup>-activating solution.

The general characteristics found for the contractility recoveries are in harmony with the results of the stiffness measurements. That is, the rate of stiffness recovery in the plain rigor solution did not show appreciable change upon transfer to the ADP-rigor solution, whereas a nearly 10 times increase in the rate was observed upon transfer to the Ca<sup>2+</sup>-rigor solution (Fig. 3, *B* and *C*). A straightforward comparison of the recovery rate of stiffness in the Ca<sup>2+</sup>-activating solution to those in the rigor solutions was obstructed by the tension-dependent compliance serial to the cross-bridges. When the apparent plateau stiffness levels attained after the prolonged incubation in the Ca<sup>2+</sup>-rigor and Ca<sup>2+</sup>-activating solutions are considered to represent the full recovery levels of stiffness in rigor and Ca<sup>2+</sup>-activating solutions, respectively, the rates of stiffness recovery can be normalized against these plateau levels (Table 2). The normalized rate in the Ca<sup>2+</sup>-activating solution was 20 times as fast as that in the plain rigor solution. (Therefore, the ratio of the recovery rates for stiffness would be plain rigor/ADP-rigor/Ca<sup>2+</sup>-rigor/Ca<sup>2+</sup>-activating = 1/1/9/20.) If some myosin heads were still in the M-ADP-analog state even after the prolonged incubation in the Ca<sup>2+</sup>-rigor solution, the ratio of 20 would be an underestimate. In any event, it is evident that the activation levels estimated from the stiffness recovery were considerably lower for the rigor solutions than for the Ca<sup>2+</sup>-activating solution.

A close inspection of Fig. 2 reveals that the slow recovery processes of contractility in rigor conditions cannot be fitted with a simple exponential or hyperbolic process asymptotic

unity. This indicates that the activation by Ca<sup>2+</sup> and rigor cross-bridges not only failed to attain full activation but also failed to recover full contractility. Coincidentally, stiffness recovery in rigor conditions showed gradual creep before reaching a plateau. These suggest that Ca<sup>2+</sup> and rigor cross-bridges can activate the myofilament only locally.

The inability of Ca<sup>2+</sup> to fully activate skeletal muscle has been claimed by several recent workers. Observing the binding of fluorescent S1 to rigor myofibrils, Swartz et al. (1996) found that the thin filament at the nonoverlap region is not fully activated even at high Ca<sup>2+</sup> concentration. Vibert et al. (1997) detected that tropomyosin in the groove on the Ca<sup>2+</sup>-activated actin filaments further moves with the formation of rigor cross-bridges. Ishiwata and Yasuda (1993) and Fukuda et al. (1998) found that a biochemical model that requires cooperative activation exerted by cross-bridges to attain full activation could successfully simulate the effects of MgATP, MgADP, and Ca<sup>2+</sup> on muscle force.

The present results not only confirmed their claims but also indicated that the activation level attained with Ca<sup>2+</sup> plus a considerable population of rigor cross-bridges is far from the activation level at fully Ca<sup>2+</sup>-activated contraction. From this, we consider that contractile cross-bridges possess prominent activating efficiency, which is indispensable to activate the entire overlap region as well as to attain the full activation level. The prominent efficiency of contractile cross-bridges compared with that of rigor cross-bridges was also reported by Güth and Potter (1987) based on the observation of the structural change induced on the fluorescence-labeled troponin C incorporated in skinned fibers.

Which cross-bridge species is responsible for the prominent activating efficiency of the contractile cross-bridges? If only the strongly bound cross-bridges have activating efficiency as commonly postulated (cf. Lehrer and Geeves, 1998), and if AM and AM-ADP during contraction are analogous to the corresponding cross-bridge species in rigor, the prominent activating efficiency can be ascribed to AM\*-ADP obtained after the P<sub>i</sub> release (see the postulated scheme of the P<sub>i</sub>- and analog-releasing mechanism shown in the Introduction). If this is the case, the AM\*-ADP obtained after the analog release would be different from the AM\*-ADP after the P<sub>i</sub> release or the population of AM\*-ADP would be too small during the analog-releasing process in the rigor solutions to cause significant additional activation. This may be related to the fact that the analogs were released without developing force (Fig. 3, *A–C*). However, we would like to reserve a possibility that weakly bound cross-bridges and/or AM-ADP and AM specific to contraction have the prominent activating efficiency. It is also possible that the force generation secondarily exerts a prominent activating effect, for instance, through the strain in the myofibrils (cf. Takemori et al., 1996).

## Assignment of activating efficiency to each activator

One can further proceed to assign activating efficiency to each activator on the assumption that the activating effects of coexisting factors simply sum up. Because the recovery rates were evaluated at the middle part of each recovery process, the difference in the population of activating cross-bridges (catalyst) and the analog-bound myosin heads (substrate) would not seriously affect the assignment. Compared with the rigor cross-bridges (AM and AM-ADP)  $\text{Ca}^{2+}$  was assigned higher efficiency for the stiffness recovery. This suggests that the actin-binding step of M-ADP-analog and the following analog-releasing step were affected differently depending on the species of activator. That is, compared with AM and AM-ADP,  $\text{Ca}^{2+}$  more strongly accelerates the actin-binding step.

The difference may possibly be related to the three states of the thin filament proposed by Vibert et al. (1997). That is,  $\text{Ca}^{2+}$  mainly accelerates binding of M-ADP- $\text{P}_i$  to actin by the removal of the steric block by tropomyosin, whereas cross-bridges accelerate the kinetics of  $\text{P}_i$  release from the AM-ADP- $\text{P}_i$  complex, which accompanies further movement of tropomyosin.

## Activating efficiency of AM-ADP

Observing the effect of ADP on the transient contraction induced by the photolysis of caged-ATP, Thirlwell et al. (1994) claimed that AM-ADP is a far more efficient activator than AM. Simulating the marked potentiating effect of MgADP observed on  $\text{Ca}^{2+}$ -free steady contraction at low [MgATP], Yamaguchi (1998) confirmed the higher activating efficiency of AM-ADP on contraction. On the other hand, Zhang et al. (1999) reported that MgADP had no significant effect on the cooperative binding of fluorescent S1 to rigor myofibrils. The present observation, which is also made in the rigor condition, showed that the activating efficiency of AM-ADP is not significantly higher than that of AM.

Because the potentiation was observed in the presence of coexisting contractile cross-bridges but not in the absence of MgATP so far as we know, we consider that the apparent contradiction described above suggests that the binding of MgADP to AM adds to the cross-bridge an ability to indirectly activate muscle through a process present only in the physiological cycling of contractile cross-bridges. In this context, it is interesting to note that the potentiation of contraction by MgADP was found to be different in nature from activation by AM and  $\text{Ca}^{2+}$  (Horiuti et al., 1997; Horiuti and Kagawa, 1998).

To clarify the activation mechanism of the contractile cross-bridges and AM-ADP in detail, additional experiments are needed.

We are grateful to Ms. Oshimoto for her technical support in the experiments and help in preparing the manuscript.

This study was supported by grants from the Uehara Memorial Foundation.

## REFERENCES

- Beck, T. W., P. B. Chase, and M. J. Kushmerick. 1992.  $^{19}\text{F}$ -NMR of the skeletal myosin subfragment-1 complex with MgADP and aluminofluoride. *Biophys. J.* 61:A435.
- Bremel, R. D., and A. Weber. 1972. Cooperation within actin filament in vertebrate skeletal muscle. *Nature N. Biol.* 238:97–101.
- Chase, P. B., D. A. Martin, and J. D. Hannon. 1994. Activation dependence and kinetics of force and stiffness inhibition by aluminofluoride, a slowly dissociating analogue of inorganic phosphate, in chemically skinned fibers from rabbit psoas muscle. *J. Muscle Res. Cell Motil.* 15:119–129.
- Chase, P. B., D. A. Martin, M. J. Kushmerick, and A. M. Gordon. 1993. Effects of inorganic phosphate analogues on stiffness and unloaded shortening of skinned muscle fibers from rabbit. *J. Physiol.* 460: 231–246.
- Danzig, J. A., and Y. E. Goldman. 1985. Suppression of muscle contraction by vanadate: mechanical and ligand binding studies on glycerol-extracted rabbit fibers. *J. Gen. Physiol.* 86:305–327.
- Danzig, J. A., M. G. Hibberd, D. R. Trentham, and Y. E. Goldman. 1991. Cross-bridge kinetics in the presence of MgADP investigated by photolysis of caged ATP in rabbit psoas muscle fibers. *J. Physiol.* 432: 639–680.
- Fukuda, N., H. Fujita, T. Fujita, and S. Ishiwata. 1998. Regulatory roles of MgADP and calcium in tension development of skinned cardiac muscle. *J. Muscle Res. Cell Motil.* 19:909–921.
- Güth, K., and J. D. Potter. 1987. Effect of rigor and cycling cross-bridges on the structure of troponin C and on the  $\text{Ca}^{2+}$  affinity of the  $\text{Ca}^{2+}$ -specific regulatory sites in skinned rabbit psoas fibers. *J. Biol. Chem.* 262:13627–13635.
- Horiuti, K. 1986. Bioassay of calcium in skinned smooth muscle by contraction of skinned skeletal muscle placed near by. *Jikeikai Med. J.* 33:149–156.
- Horiuti, K., and K. Kagawa. 1998. Effects of ADP and low ATP on the  $\text{Ca}^{2+}$ -sensitive transient contraction upon photolysis of caged ATP in rat muscle fibers: a study on the Bremel-Weber type cooperation. *J. Muscle Res. Cell Motil.* 19:923–930.
- Horiuti, K., N. Yagi, and S. Takemori. 1997. Mechanical study of rat soleus muscle using caged ATP and x-ray diffraction: high ADP affinity of slow cross-bridges. *J. Physiol.* 502:433–447.
- Ishiwata, S., and K. Yasuda. 1993. Mechano-chemical coupling in spontaneous oscillatory contraction of muscle. *Phase Transit.* 45:105–136.
- Lehrer, S. S., and M. A. Geeves. 1998. The muscle thin filament as a classical cooperative/allosteric regulatory system. *J. Mol. Biol.* 277: 1081–1089.
- Marston, S. B., C. B. Rodger, and C. T. Tregear. 1976. Changes in muscle crossbridges when  $\beta,\gamma$ -imido-ATP binds to myosin. *J. Mol. Biol.* 104: 263–276.
- Maruta, S., G. D. Henry, B. D. Sykes, and M. Ikebe. 1993. Formation of the stable myosin-ADP-aluminum fluoride and myosin-ADP-beryllium fluoride complex and their analysis using  $^{19}\text{F}$  NMR. *J. Biol. Chem.* 268:7093–7100.
- Natori, R. 1954. The role of myofibrils, sarcoplasm and sarcolemma. *Jikeikai Med. J.* 1:18–28.
- Shoenberg, M., and E. Eisenberg. 1987. ADP binding to myosin cross-bridge and its effect on the cross-bridges and its effect on the cross-bridge detachment rate constant. *J. Gen. Physiol.* 89:905–20.
- Shimizu, H., T. Fujita, and S. Ishiwata. 1992. Regulation of tension development by MgADP and  $\text{P}_i$  without  $\text{Ca}^{2+}$ : role in spontaneous tension oscillation of skeletal muscle. *Biophys. J.* 61:1087–1098.
- Smith, R. M., and A. E. Martell. 1974–1982. Critical Stability Constants, Vols 1–5. Plenum Press, New York.

- Swartz, D. R., R. L. Moss, and M. L. Greaser. 1996. Calcium alone does not fully activate the thin filament for S1 binding to rigor myofibrils. *Biophys. J.* 71:1891–1904.
- Takemori, S., M. Yamaguchi, and Y. Umazume. 1996. Physiological significance of viscoelastic structures in myoplasm. *Adv. Biophys.* 33: 151–157.
- Takemori, S., M. Yamaguchi, and N. Yagi. 1995a. An x-ray diffraction study on a single frog skinned muscle fiber in the presence of vanadate. *J. Biochem.* 117:603–608.
- Takemori, S., M. Yamaguchi, and N. Yagi. 1995b. Effects of adenosine diphosphate on the structure of myosin cross-bridges: an x-ray diffraction study on a single skinned frog muscle fiber. *J. Muscle Res. Cell Motil.* 16:571–577.
- Thirlwell, H., J. E. T. Corrie, G. P. Reid, D. R. Trentham, and M. A. Ferenczi. 1994. Kinetics of relaxation from rigor of permeabilized fast-twitch skeletal fibers from the rabbit using a novel caged ATP and apyrase. *Biophys. J.* 67:2436–2447.
- Vibert, P., R. Craig, and W. Lehman. 1997. Steric-model for activation of muscle thin filaments. *J. Mol. Biol.* 266:8–14.
- Yamaguchi, M. 1998. Modulating factors of calcium-free contraction at low [MgATP]: a physiological study on the steady states of skinned fibers of frog skeletal muscle. *J. Muscle Res. Cell Motil.* 19:949–960.
- Zhang, D., K. W. Yancey, P. Sanghani, and D. R. Swartz. 1999. Effect of ADP on the activation of the thin filament by cross-bridges in myofibrils. *Biophys. J.* 76:A155.